Fatigue properties of a semi-solid cast Al-7Si-0.3Mg-T6 alloy

***C. J. Davidson, *J. R. Griffiths, **M. Badiali and **A. Zanada**
***CSIRO Manufacturing Science and Technology - Kenmore - Australia**
****Teksid S.p.A. Divisione Alluminio - Carmagnola (Torino) - Italy**

Abstract

The room temperature fatigue properties of a semisolid cast A356 alloy have been defined by determining a Wšhler curve for lives between 10^4 and 10^7 cycles. The fatigue tests were carried out in axial tension/compression cycling at zero mean stress (stress ratio, R, of -1). The initiation sites of the fatigue cracks were studied in detail and it was observed that cracks generally initiated from shrinkage pores or oxide films at the surfaces of the machined fatigue specimens. Measurements of the sizes of these defects are reported, and evidence is presented to suggest that oxide defects have less effect on the fatigue life than shrinkage pores of the same size, presumably reflecting differences in the ease of fatigue crack initiation at the two types of defects. The fatigue properties of our particular semisolid castings are compared with those of casting made by other processes. It is shown that the semisolid castings performed slightly better than squeeze castings made in our laboratory using the same machine and the same die. The properties of both the semisolid and squeeze castings are significantly better than those of gravity diecastings.

Keywords

Fatigue, defects, oxides, porosity.

Riassunto

Le proprietà a fatica a temperature ambiente di una lega A356 semisolida sono state definite tramite la determinazione di una curva di Wöhler per durate di 10^4 a 10^7 cicli. Le prove di fatica sono state eseguite in cicli di tensione/compressione assiale a sollecitazione media zero (rapporto di sollecitazione, R, -1). L'analisi dettagliata delle zone di innesco delle cricche da fatica ha dimostrato che quest'ultime tendono a partire da porosità da ritiro o da strati sottili di ossidi. Vengono riportate le dimensioni di tali difetti. Si ipotizza che gli ossidi influenzino meno la durata a fatica che non le porosità da ritiro di pari dimensioni, il che riflette presumibilmente le differenze tra la suscettibilità allo sviluppo iniziale di una cricca da fatica a livello dei due tipi di difetto. Le proprietà a fatica dei getti semisolidi vengono confrontate con quelle di getti realizzati con altre tecnologie. Si è potuto osservare che il comportamento dei getti semisolidi era leggermente migliore di quello di getti tipo "squeeze" colati con la stessa macchina e con la stessa forma nel nostro laboratorio. Le proprietà di questi getti semisolidi e squeeze sono significativamente migliori di quelle di getti colati in conchiglia per gravità.

Parole chiave

Datica, difetti, ossidi, porosità.

INTRODUCTION

It has long been known that the fatigue endurance of castings is sensitive to the size of casting defects [1]. There is some evidence that it is also affected, but to a lesser extent, by solidification time as reflected by dendrite arm spacing and the size of silicon particles [2, 3]. The porosity of semisolid castings can be very low and so the process should be capable of providing castings that have superior fatigue properties. Surprisingly, however, there are few references to the fatigue properties of such castings although semisolid casting has been promoted as a "high integrity" casting process for at least 20 years. Indeed, we are aware of only three pieces of work [4, 5, 6] and the results from reference 4, in particular, suggest that the process can confer a greatly enhanced fatigue performance.

In this paper we report observations on the microstructure and mechanical properties (tensile and fatigue) of semisolid castings made in the CSIRO foundry using Al-7Si-0.3Mg alloy. The properties of the semisolid castings are compared with those of squeeze castings and gravity diecastings using alloys of essentially the same composition.

EXPERIMENTAL METHODS

Materials

Thixotropic billets were supplied by Aluminium Pechiney. The composition of the castings was found by ICP-AES (Inductively Coupled Plasma / Atomic Emission Spectrometry) and is shown in Table 1. The composition conforms to the United States Aluminum Association specification for A356 with the addition of Sr as a chemical modifier.

Design of castings, casting procedure and heat-treatment

A stepped plate casting (Fig. 1) was used for this work, casting being carried out in an Ube horizontal die-clamping, vertical injection, squeeze casting machine, which applied a squeeze pressure of 100 MPa soon after the cavity was filled. The operational conditions have been described elsewhere [7]. The 10 mm and 15 mm steps were cut from the plates and were given a T6 heat-treatment of 6 hours at 540°C, followed by quenching into water at 25°C, natural ageing for 20 hours and, finally, artificial ageing for 6 hours at 170°C. This produced a slightly under-aged condition.

Specimen design, tensile tests and hardness tests

The heat-treated bars were machined into cylindrical tensile and fatigue test specimens. Tensile specimens had a gauge length of 20 mm and a gauge diameter of 5 mm. Tensile tests were made using a screw-driven machine, the strains being measured with an extensometer. Fatigue specimens had the same design except that they had a 10 mm gauge length to avoid buckling in compression. Vickers hardness measurements were made on the grip ends of selected specimens after testing.

Fatigue tests

Tests were carried out in a servo-hydraulic machine in sinusoidal force control. All tests were done at a stress ratio, R, of -1 (i.e., zero mean stress). The ambient temperature varied between 22 and 26°C and the relative humidity was usually between 30% to 40%. Care was taken to align the load train and evidence of the good alignment was that the locations of the fracture origins with respect to the load frame were random over the course of these experiments.

Microstructure and fractography

Optical metallographic observations were made of the cast microstructure. In addition, the fatigue fracture surfaces were examined in a low-power stereomicroscope for evidence of defects near the initiation site. Some fracture surfaces were also examined by scanning electron microscopy using secondary electron imaging and light-element energy-dispersive X-ray spectroscopy.

Table 1 - Chemical composition of the castings (wt%)

Si	Mg	Fe	Sr	Ti	Mn	Zn
6.4	0.35	0.11	0.024	<0.005	<0.01	0.02

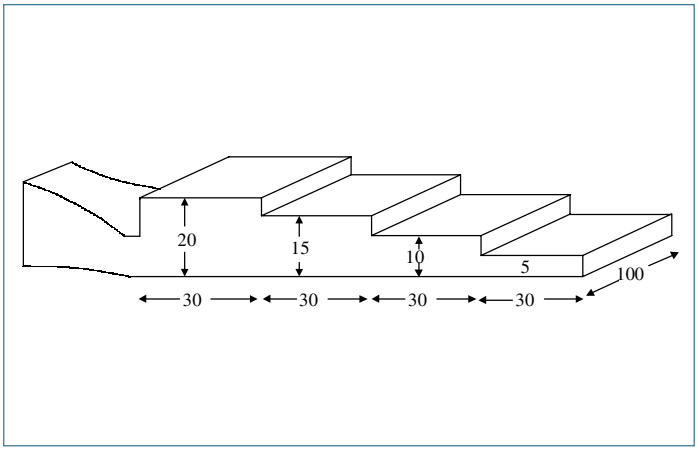

Fig. 1: The cast plate (ingate on left-hand side)

RESULTS

Metallography

The microstructure was typical of semisolid castings [7] and no differences could be observed between the 10, 15 and 20 mm thick sections of the plates. The 5 mm section did contain some subsurface oxide films and evidence of unsteady filling, but in any case was too thin to be used to prepare test samples. The 20 mm section generally showed some slight shrinkage porosity in X-radiographs and so these sections were also not used for fatigue samples.

Tensile and hardness properties

The tensile and hardness properties of the heat-treated castings are shown in Table 2 and are typical of the properties for A356 alloy heat-treated to a T6 condition.

Table 2 - Tensile and hardness data (mean ± estimated standard deviation)

0.2% proof stress (MPa)	tensile strength (MPa)	elongation to fracture, %	Vickers hardness (10 kgf)
267±5	321±3	15±3	114±2

Fatigue tests

The results of the fatigue tests are shown in Fig. 2. The data points are separated to show results from specimens cut from the 10 mm and 15 mm steps. The lines drawn on this Figure are taken from the Design Guidelines for Squeeze Castings [8] and are included here for later reference in the Discussion. The lines represent estimated stresses for 10%, 50% and 90% probabilities of survival. Our tests were terminated at 10^7 cycles, the fatigue strength at this life being determined by testing 15 specimens using the "staircase" procedure [9]. Not enough specimens were available to test the 10 mm and 15 mm steps separately, but when the data from both the 10 and 15 mm steps were combined, the 50% survival stress at 107 cycles was 135 MPa; the 10% and 90% survival stresses were 143 and 127 MPa, respectively.

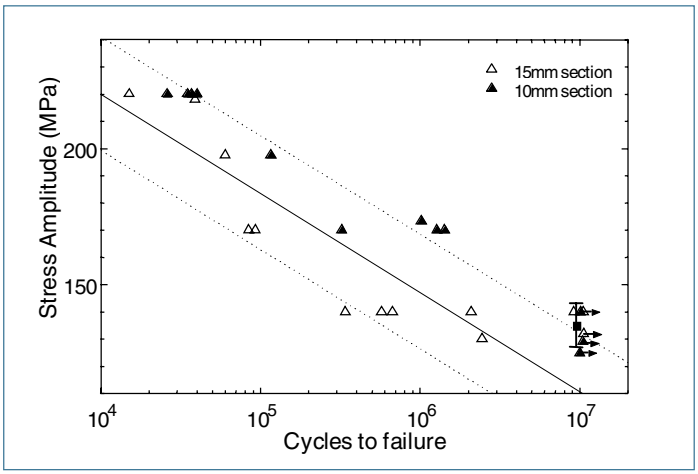

Fig. 2: S-Nf data for semisolid-cast plates. The point with the error bars at 107 cycles is the result from the staircase analysis

Fractography

The fracture surfaces were examined as described in above and in all but 6 of the 30 specimens examined it was possible to identify a casting defect at the crack origin. Of the 24 identified defects, 12 were probably oxide films and 12 were shrinkage pores. The area of each defect was measured and the observations are summarised in Table 3 and Table 4. The absolute range of defect sizes in this dataset was from 2 700 µm2 to 190 000 µm2.

Table 3 - Summary of defects that initiated fatigue failures (overall numbers)

	type of defect		
	pores	oxides	unresolved
number	12	12	6
mean area (µm²)	51 000	29 000	
median area (µm²)	24 000	21 000	

Table 4 - Summary of defects that initiated fatigue failures (sorted by position in casting). The unresolved defects were assumed to have zero size for the purposes of these calculations

step height	type of defect (mm)			area of defect µm2	
	pores	oxides	unresolved	mean*	median*
10	1	8	5	13 000	10 000
15	11	4	1	49 000	30 000

DISCUSSION

Fractography

Two things are apparent from Table 3 and Table 4. First, the critical defects in the 10 mm step were significantly smaller than those in the 15 mm step. Second, the defects in the 10 mm step tended to be oxide films whereas those in the 15 mm step tended to be shrinkage pores. It cannot necessarily be inferred from Table 4 that oxides are more prevalent in the 10 mm step. An alternative, and more plausible, interpretation of the data is that the shrinkage pores are smaller in the 10 mm step while the oxide film fragments have similar sizes in the two steps. Larger shrinkage pores are more likely to be formed in the thicker sections because solidification will take longer there and feeding through the gate becomes more difficult as solidification progresses.

There are three possible sources of oxide films: (a) the exposed surface of the billet during heating; (b) the fresh surfaces exposed during filling and then folded back in; and (c) films stirred in during manufacture of the thixotropic billets by DC casting. Only 20% of the oxides identified as initiating fracture were of the thick type, characteristic of fragments from the billet surface. The remainder were much thinner, typically well below the electron penetration depth in the SEM, and they were probably of the order of 0.1 µm in thickness.

No initiating defect was found in 6 of the 30 specimens examined. The smallest defect observed in this work had an area of 2700 µm² and one possibility for the "defect-free" specimens is that the defects simply could not be seen, either because the defect size was less than the limit of resolution of the optical system or they gave insufficient contrast. An alternative possibility is that the figure of ~2000 µm² is a lower limit beyond which, as suggested by others [10, 12], other fatigue crack initiation mechanisms come into operation. If this second alternative is true then the observed fatigue limit of ~135 MPa is close to the limit for this alloy, regardless of further decreases in casting defect size.

The fatigue properties of semisolid castings and those of squeeze and gravity diecastings

Questions are often asked about mechanical properties characteristic of particular casting techniques, and design curves are produced purporting to show the fatigue properties of alloys cast by a particular method. An example is the design curve for squeeze castings shown in Fig. 2. This shows that our data for semisolid castings are consistent with current accepted practice for squeeze casting. However, as has been known for 50 years [1], a database for the fatigue properties of a particular alloy should contain size estimates for the defect population as well as the usual details of composition and heat-treatment condition. To illustrate this we summarise in Table 5 some of our work on the fatigue strengths of Al-Si-Mg castings made by squeeze casting [13] and by gravity diecasting [11] and compare them with the present data for semisolid castings. The alloys were modified with Sr to match the semisolid feedstock. The castings were all made as plates identical to that shown in Fig. 1 and they were heat-treated to a T6 condition.

Table 5 - Fatigue strengths of Al-Si-Mg-T6 castings at 10^7 cycles at R = -1 for three casting methods

casting method	alloy composition wt% Mg	Fe	proof stress MPa	fatigue strength MPa	dominant defect type	median defect area µm²	reference
semisolid	0.35	0.11	267	135	oxide/porosity	20 000	this paper
squeeze	0.36-0.37	0.13	267	130	oxide	40 000	13
gravity	0.28-0.34	0.12-0.20	234	111	porosity	80 000	11
gravity	0.61-0.90	0.11-0.16	323	110	porosity	80 000	11

The data in Table 5 conform qualitatively to the concept that the fatigue strength increases as the defect size decreases. They also show the marked improvement in the two "high integrity" castings compared with gravity diecasting. However the quantitative agreement with the scaling rule described below in ¤4.3 between fatigue strength and defect area is only moderate and possible reasons for this are given below.
4.3 The S-Nf fatigue relation for castings - effects of defect size and defect type. Fig. 2 shows that the fatigue strength of specimens cut from the 10 mm step is approximately 20 MPa higher than for the 15 mm specimens. This can be explained qualitatively by the fact that the defect sizes were smaller in the 10 mm step. A quantitative relationship between the fatigue life, N_f, the stress amplitude, a_a, and a length dimension, a_i, which characterises the size of the defect can be found by integrating the Paris Equation for fatigue crack growth [12, 13, 14, 15]. An approximate solution is

$$\sigma^m_a N_f a_i^{(m-2)/2} = B \qquad (1)$$

in which m is the Paris exponent and the constant, B, includes the Paris Law pre-exponential term and various other terms including the assumed relation between the stress amplitude and the effective stress. We assume that $m = 4$ [12] and, since A_i, the defect area, is proportional to a^2_i, it follows that

$$\sigma^4_a N_f A_i^{1/2} = B' \qquad (2)$$

in which B' includes the constant of proportionality between a_i and A_i. The amount of data presented in this paper is insufficient to test Equation 2 and, in any case, such tests have been made many times in the past. However, an interesting

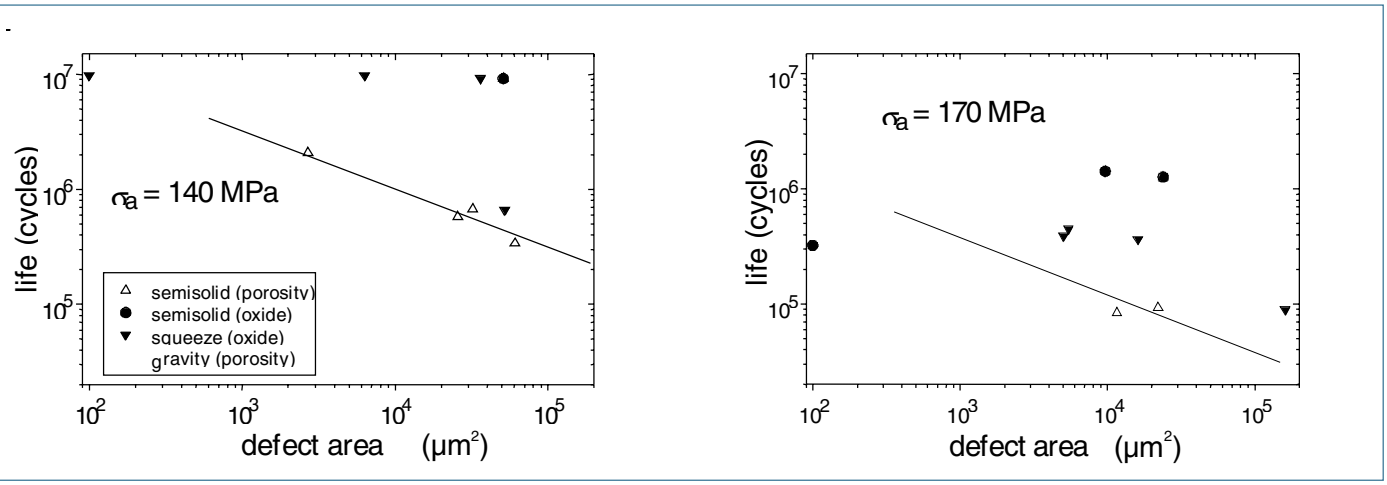

Fig. 3: Fatigue life and defect size for two stress amplitudes and three casting methods (semisolid data have been separated according to type of defect). The reference line has a slope of -0.5. The semisolid casting with a life of $3x10^5$ cycles had no observed defect and was given an arbitrary area of 99 µm².

Three things can be seen from the Figure. First, when fatigue cracks initiate at pores (open symbols) a single relation between N_f and Ai appears to hold regardless of casting method - and, moreover, is consistent with Equation 2 (Fig. 2 shows that scatter in the S-N diagram is reduced at high stresses and it may be that the fatigue life is much less sensitive to defect size under such conditions). Second, when cracks initiate from oxide films the data have a very large scatter but, importantly, there is a consistent trend showing that oxide films generally have a smaller effect on fatigue life than do pores of the same area. Third, the prediction that the fatigue strength at a given defect size should be proportional to σ^{-4} does not hold very well for the two stresses reported here even when initiation only from shrinkage pores is considered. (For example, consider a defect area of 10^5 μm^2. At 140 MPa N_f is ~$3x10^5$ cycles while at 170 MPa it is ~$4x10^4$ MPa. The ratio of lives is ~7.5 while $(170/140)^4$ is only ~2.2). The first of these observations, while new, is unexceptional, merely showing that shrinkage pores have the same effects in gravity diecastings as in semisolid castings. The second observation is interesting. It suggests that fatigue crack initiation is more difficult from oxide films than from pores. It is believed that initiation from pores starts at, essentially, the first fatigue stress cycle [14] but the present data suggest there is a significant initiation life, or incubation period, in the case of oxide films. A possible reason for this difference is that the oxides may adhere to the Al matrix and thereby reduce the stress concentration factor at their edges compared to pores of the same size, but further work is required to test this hypothesis. The third effect (that the fatigue strength does not conform to the scaling rule of Equation 2) appears significant and is, as yet, not properly explained. The problem may be a result of the small amount of data or because the parameters in the fatigue crack growth law (including the threshold stress intensity factor and crack closure effects) have not been evaluated for the microstructures associated with the different casting techniques.

CONCLUSION

The following conclusions can be made regarding the fatigue strength of 356-T6 castings made by semisolid and other processes:

(i) The fatigue strength of semisolid castings is determined by either oxides or pores. Oxides and pores were observed to initiate fatigue cracks with equal frequency.

(ii) The initiating defects in semisolid castings were somewhat smaller than the oxide films in squeeze castings made in the same machine.

(iii) The fatigue strengths of semisolid castings made for this project were similar to those of squeeze castings made in the same die. In this particular case, the semisolid castings were slightly superior.

(iv) A single relation between fatigue life and pore area holds for both semisolid and gravity diecastings at moderate stress amplitudes.

(v) The life/size data for initiation from oxides are widely scattered compared to pore-initiated fatigue. However, there is a significant trend showing that oxide defects have less effect on fatigue life than do pores of the same area.

REFERENCES

1 N. E. Promise, Evaluation of non-ferrous materials (1956), cited by H. E. Boyer in Atlas of Fatigue Curves, American Society of Metals, (1960).

2 T. L. Reinhart, ASM Handbook, 19, (Fatigue and Fracture), (1996), p.813-822.

3 W. Chen, B. Zhang, T. Wu, D. R. Poirier and Q. T. Fang, Materials Solutions Conference, ASM International, (1998).

4 J-P. Gabathuler, H. J. Hubner and J. Erling, Proc. Int. Conf. On Aluminium Alloys:New process technologies, Marina di Ravenna, AIM, (1993), p. 169-180.

5 B. Bieri, P. J. Uggowitzer, T. Imwinkelried, J-P. Gabathuler and M. O. Spiedel, Proc. 4th. Decennial Conf. on Solidification Processing, Sheffield, (1997), p. 625-629.

6 J-P. Gabathuler, R. Jaccard, E. Ršllin and Ch. Ditzler, Eigenschaften von Bauteilen aus Aluminium, hergestellt nach dem Thixoforming-Verfahren, VDI Berichte Nr. 1235, (1995), p. 81-106.

7 Z. W. Chen, S. J. Peck and C. J. Davidson, Int. J. Cast Metals Research, 12, (1999), p.127-135.

8 Design Guidelines for Squeeze Castings, ed. R. Zehe, Elm Publications, (1994).

9 W. Maennig: Planning and evaluation of fatigue tests, ASM Handbook, 19 (Fatigue and Fracture), ASM International, (1996), p. 303-313.

10 H. Kitagawa and S. Takahashi, Proc. 2nd. Int. Conf. on Mech. Behavior of Materials, pub. ASM, (1976), p. 627-631. Also S. Suresh, Fatigue of Materials, Cambridge University Press, (1991), p.297.

11 C. J. Davidson and J. R. Griffiths, CSIRO Internal Report CMST-B-98-28, (1999).

12 M. J. Couper, A. E. Neeson and J. R. Griffiths, Fatigue and Fracture of Engng. Mater. Struct., 13, (1990), p.213-227.

13 C. J. Davidson, J. R. Griffiths and C. Wang, Proc. Conf. on Fracture Mechanics and Advanced Eng. Materials, eds. Lin Ye and Yiu-Wing Mai, pub. University of Sydney, (1999), p.217-224.

14 B. Skallerud, T. Iveland and G. HŠrkegŒrd, Engng. Fract. Mechanics, 44, (1993), p.857-874.

15 J. F. Knott, Proc. 3rd. Int. Conf. on Fatigue and Fatigue Thresholds, "Fatigue '87", eds. R. O. Ritchie and E. A. Starke, pub. EMAS, (1987), p.497-515.